



ELSEVIER

Field Crops Research 43 (1995) 67–76

**Field  
Crops  
Research**

## Water uptake by pearl millet in a semiarid environment

B.D. McIntyre<sup>a</sup>, S.J. Riha<sup>a,\*</sup>, D.J. Flower<sup>b</sup>

<sup>a</sup> Department of Soil, Crop and Atmospheric Sciences, Cornell University, Ithaca, NY 14853, USA

<sup>b</sup> International Crops Research Institute for the Semi-Arid Tropics (ICRISAT), Patancheru, Andhra Pradesh 502 324, India

Received 18 November 1994; accepted 22 June 1995

### Abstract

Crops during drought may not utilize water at depth. This under-utilization of deep water may result from slow rates of root extension, low root density, or a decline in soil water potential or associated phenomena. The importance of several of these factors on pearl millet (*Pennisetum glaucum* (L.) R. Br., cv. CIVT) water uptake and growth from panicle initiation to flowering was studied on a sandy soil in northern Nigeria during two dry seasons. Half of the crop was irrigated while the other half received no water after panicle initiation. Soil water content, stomatal conductance and stem extension were measured periodically.

A potential-driven water uptake model, which assumes a static, exponential distribution of roots and couples transpiration to leaf water potentials, described in both seasons the observed pattern and timing of water uptake, as well as predawn leaf water potential and actual transpiration. As the soil dried, estimated transpiration declined below potential transpiration and modeled and measured predawn leaf water potential declined. There was close agreement between observed and modeled predawn leaf water potential and soil water uptake. Analysis using the model indicated that decreased water uptake at depth was attributable to root distribution throughout the soil profile, as well as to low root length density at depth.

**Keywords:** Millet; Modelling; *Pennisetum glaucum*; Root distribution; Stomatal conductance; Transpiration; Water extraction

### 1. Introduction

Analyses of the water uptake of crops subjected to extended drought indicate that many crops appear to under-utilize water in the lower depths of the soil profile (Passioura, 1983). This phenomenon has been noted by several researchers, e.g., Barraclough and Weir (1988), and has been variously attributed to low root density at depth (Jordan and Miller, 1980; Robertson et al., 1993a), the onset of crop maturity before deep water extraction commences (Robertson et al., 1993a), uneven root distribution, and high root axial resistance

to water flow (Passioura, 1983; Hamblin and Tennant, 1987).

Under-utilization of deep water is of particular interest in the sandy soils of the millet-growing regions of West Africa ( $> 11^{\circ}50'N$ ), which usually receive less than 750 mm of unimodally distributed rainfall per year (Kowal and Knabe, 1972). Crops in this zone are often subjected to protracted lapses between rainfall events. Under these conditions, under-utilization of deep water could substantially limit crop growth and yield.

To study the under-utilization of deep water by pearl millet, the rate and extent of stored soil water uptake were measured in field experiments. The crop was irrigated until panicle initiation in order to ensure establishment and vigorous root growth. After panicle

\* Corresponding author.

initiation, water was withheld from half the crop while irrigation continued on the other half. Water uptake patterns in the drought treatment were analyzed with a potential-driven water uptake model (Campbell, 1985). In this model, plant water potential is a function of the transpiration rate and the rate of water flow to roots. As plant water potential changes, transpiration changes as a function of the impact of plant water potential on stomatal conductance. With this potential-driven approach, the impact of both above- and below-ground processes on water uptake can be considered.

## 2. Materials and methods

### 2.1. Experimental site, design, and cultural practices

Research was conducted at the Kano substation of the International Institute for Tropical Agriculture (IITA) on experimental plots in Minjibir, Nigeria (12°8'N, 8°40'E; 500 m asl). The site is well-drained with 0 to 1% slope and the soil is a hypothermic, ustic Plinthic Quartzipsamment (USDA taxonomy) comprised of 86% sand, 7% silt, and 7% clay. Bulk density was 1.6 Mg m<sup>-3</sup> throughout the profile with an ironstone layer occurring between 1.0 and 1.2 m. The pH of the soil in water was slightly acidic ranging from 6.1 at the surface to 6.7 at 1 m. Organic matter (carbon lost on ignition) ranged between 1.1% at the surface to 2.2% at 1 m.

Both experiments took place during dry seasons. Climatic conditions occurring during the two experiments are presented in Table 1. Irrigated plots were separated from nonirrigated plots by approximately 18 m to prevent lateral movement of water into the nonirrigated area. There were four replications. Plot size was 6 × 5 m. A 3-m border of maize surrounded the experimental plots.

Plots were disc-harrowed and then raked level by hand. Fertilizer (30 kg N, 13 kg P, and 25 kg K ha<sup>-1</sup>) was broadcast prior to sowing. Three to six seeds were sown per hill in 0.75-m rows with an in-row spacing of 0.25 m. After thinning to one plant per hill 2 weeks after sowing, the final density was 53 300 plants ha<sup>-1</sup>. This stand density is commonly used for millet by the Institute for Agriculture Research, Zaria, Nigeria. Weeding was done by hand as required.

Table 1

Sowing date, mean daily climatic conditions, and mean daily potential evapotranspiration and mean daily estimated transpiration during two 18-day experimental periods in northern Nigeria

Variables	Expt 1	Expt 2
Sowing date	10 Oct 89	28 Mar 90
Temperature (°C)		
Air (2 m)	22	32
Soil (0.05 m)	23	34
Vapor pressure deficit (kPa)	3.7	5.2
Solar radiation (MJ m <sup>-2</sup> day <sup>-1</sup> )	20	22
Potential evapotranspiration, ET* (mm day <sup>-1</sup> ) <sup>a</sup>	6.3	9.2
Estimated transpiration, T (mm day <sup>-1</sup> ) <sup>b</sup>	3.8	4.2

<sup>a</sup>Penman–Monteith equation.

<sup>b</sup>Estimated from soil water depletion.

Crops were irrigated with sprinklers on a 3- to 4-day schedule to replace water lost to evapotranspiration. Irrigation was withheld from nonirrigated plots at the beginning of GS2 (panicle initiation, as determined by dissection) in Expt 1 and 7 days after panicle initiation in Expt 2 (21 and 33 days after sowing, respectively). The last day of irrigation on the henceforth nonirrigated plots is referred to as Day 0. Irrigation on the control plots continued on a 3- to 4-day schedule until the experiments were concluded on Day 18.

Seed of pearl millet (cv. CIVT; this acronym stands for Composite Intervarietal de Tarna, a composite developed at Tarna by Niger's national program) were obtained from the ICRISAT (International Center for Crops Research in the Semiarid Tropics) Sahelian Center (Niamey, Niger). This cultivar requires 50 to 55 days for flowering and is suited to the Sudano–Sahelian environment.

### 2.2. Measurements

Soil water content ( $\theta$ ) was measured daily, beginning at 0700 h on plots assigned to the nonirrigated treatment. The surface 0.20 m was measured gravimetrically with a piston-type corer. A neutron probe (Didcot Instrument, Oxford, UK) was used to measure water content every 0.15 m throughout the profile until the ironstone layer was reached (approximately 1.2 m). Four aluminum access tubes (16 tubes per treatment) were installed in each plot. Two of the four access tubes were within rows (midway between

plants) and two were midway between rows. Data presented are means of measurements made from all four tubes. Because soil evaporation was determined to be negligible by 2 to 4 days after an irrigation (McIntyre, 1992), transpiration was estimated as the daily water loss from the entire profile as measured with the neutron probe. Estimated transpiration and potential transpiration are reported as 3-day running means. Upper and lower limits of extractable soil water (from 0 to 1.12 m) were determined to be 193 mm and 51 mm, respectively (McIntyre, 1992).

Air temperature, relative humidity, wind speed and incoming solar radiation were measured every 5 min and hourly averages were recorded. The sensors were located approximately 10 m from the plots and 2 m above the ground. Photosynthetically active radiation was measured mid-day above and below the canopy with a 0.8-m linear probe comprised of 80 sensors at 0.01-m intervals (Sunfleck Ceptometer, Decagon Devices, Pullman, Washington) in Expt 2 and in the beginning of Expt 1. After the first 10 days of Expt 1, intercepted radiation was predicted from leaf area index measurements (McIntyre et al., 1993). Potential evapotranspiration ( $ET^*$ ) was calculated from hourly averages using the Penman–Monteith equation.  $ET^*$  was then multiplied by the measured fraction of radiation intercepted by the canopy to estimate potential transpiration ( $T^*$ ).

After irrigation was terminated on the drought treatment, predawn leaf water potential ( $\Psi_{\text{leaf}}$ ) was measured with a pressure chamber (PMS, Corvallis, Oregon) on both irrigated and nonirrigated plots. The measurements were made every 3 days between 0400 and 0530 h on young, fully expanded leaves from four plants per plot. Leaves were cut, wrapped in plastic film and transported to the pressure chamber. Measurements were made within minutes of excision from the plant. Stomatal conductance was measured daily between 1300 and 1400 h on young, fully expanded and exposed leaves of six plants per plot with a calibrated transient porometer (FET MK3, Delta-T Devices, Cambridge, UK).

Stem + leaf extension (hereafter referred to as stem extension) was measured daily on seven plants in each plot. Metal pegs secured in the ground provided a consistent reference height and the length was measured from leaf tip to reference. When a new leaf emerged from the whorl, the older leaf was measured for the

final time and measurements commenced on the new leaf. This procedure provided a continuous measurement of extension rate.

Four 0.15-m  $\times$  0.55-m  $\times$  0.15-m soil samples were taken in 0.15-m depth increments (two samples within rows and two between rows) to a total depth of 1.05 m in each plot to estimate root length density ( $L$ ). Samples were collected on Day 4 to 7 in Expt 1 and Day 3 to 6 in Expt 2. Roots were separated from the soil by washing the soil through sieves and root length was determined with a Comair scanner (Commonwealth Aircraft, Melbourne, Australia).  $L$  is reported as the average of all four samples at a given depth increment.

### 3. Simulation model

#### 3.1. Description of the model

The basic structure and implementation of the model used in this study were presented in detail by Campbell (1985). In the model, root water uptake is considered directly proportional to the potential gradient between the soil and root xylem and inversely proportional to the sum of soil and radial root resistances (Gardner, 1965). Soil resistance assumes a cylindrical flow of water to the roots that varies with  $L$ , root diameter, and soil hydraulic conductivity (Cowan, 1965). Soil hydraulic conductivity is a function of soil water potential. The soil is divided into layers so that  $L$  may be varied with depth and soil water potential may vary with depth and time. Therefore, soil resistance can change with both soil depth and time.

Root xylem water potential is calculated from  $T^*$ , root and soil resistances, and soil water potentials using the approach of Childs et al. (1977). No lower limit is set for leaf or root xylem water potential. Stomatal conductance is assumed to decrease as leaf water potential declines (Fisher et al., 1981). This function is in turn used to lower the transpiration rate in the next time step (Stockle and Campbell, 1985; Buttler and Riha, 1992).

#### 3.2. Implementation

The following values were taken from Campbell (1985) as inputs for the plant component of the model:  $R_r$  (root resistance per unit root length) =  $2.5 \times 10^{10} \text{ m}^4$

$s^{-1} \text{ kg}^{-1}$ ,  $R_L$  (leaf resistance) =  $2 \times 10^6 \text{ m}^4 \text{ s}^{-1} \text{ kg}^{-1}$  and  $\Psi_{\text{crit}} = -1.5 \text{ MPa}$ . Values for root length were derived from experimental data, which indicated an exponential decline with soil depth below the surface 0.15 m:

$$L_z = L_0 \exp(-\alpha z),$$

where  $L_z$  is the density at depth  $z$ ,  $L_0$  is the surface (0–0.15 m) density, and  $\alpha$  is the reciprocal of the depth at which  $L_z$  is 63% of the surface  $L_0$  (Gerwitz and Page, 1974).  $L_0$  was not measured because of organic matter contamination. Rather it was assigned a value of  $5 \times 10^4 \text{ m m}^{-3}$  as in Campbell (1985). The decline in measured  $L$  with depth in the profile below the surface 0.15 m was described well with  $\alpha = 3.5 \text{ m}^{-1}$  (data not presented). Values of  $L_z$  for each layer of the profile were held constant over the time of the simulation. Rooting depth was also not increased during the simulation because at the time simulation began (Day 0; onset of GS2), roots existed to a depth of approximately 1 m in Expt 1 and 0.7 m in Expt 2.

Soil hydraulic properties were obtained from soil moisture release curves of the experimental soil fit to  $\Psi_m = \Psi_e (\Theta/\Theta_s)^{-b}$  where  $\Psi_m$  and  $\Psi_e$  are, respectively, the soil matrix and air-entry water potentials,  $\Theta_s$  is the saturated soil water content, and  $b$  is the slope of  $\ln \Psi$  versus  $\ln \Theta$ . A value of 2.4 was used for  $b$  and  $-2.7 \text{ J kg}^{-1}$  used for  $\Theta_e$  for all soil depths. Upper drained limit was determined through water content measurements made during the rainy season and then used in the model to derive saturated hydraulic conductivity ( $1 \times 10^{-4} \text{ kg s m}^{-3}$ ).

## 4. Results

### 4.1. Environmental conditions

The mean daily receipt of short wave radiation was similarly high in both experiments as the result of relatively cloud-free skies (Table 1). Mean  $ET^*$  was 46% greater in Expt 2 than in Expt 1 (Table 1), however, due to advective conditions. Crops in the nonirrigated plots were forced to rely on stored soil water in an increasingly dry profile because no rainfall occurred during the experimental periods.

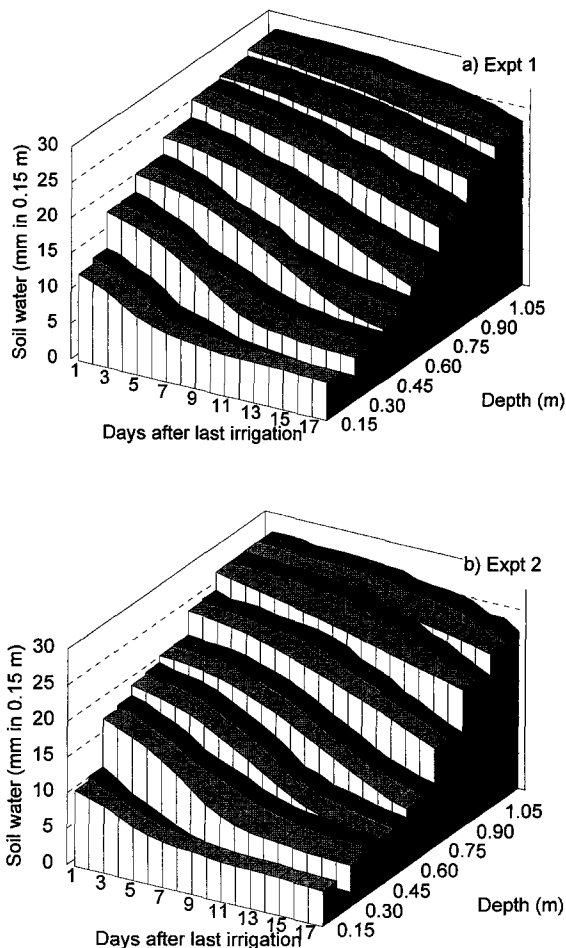


Fig. 1. Simulated (light bar) and measured (dark bar) changes in soil water for 0.15-m layers centered at depths 0.15, 0.30, 0.45, 0.60, 0.75, 0.90 and 1.05 m in (a) Expt 1 and (b) Expt 2.

### 4.2. Soil water content

Although mean  $ET^*$  was 46% greater in Expt 2 than in Expt 1, mean estimated transpiration (i.e., measured soil water depletion) differed between the two experiments by only 10% (Table 1). By Day 18 in both experiments roots had reached 1.0 to 1.2 m, but measured water uptake was not much greater below 0.9 m in Expt 2, compared to Expt 1, despite greater  $ET^*$  (Fig. 1).

Measured soil water content with depth and time followed similar patterns in both experiments. Soil water content declined most rapidly in soil layers closest to the surface, with uptake at depth lagging behind. In general, predicted soil water content with depth fol-

lowed a similar pattern (Fig. 1). Regression of predicted values against measured data for all soil depths indicated a high degree of correlation ( $r^2=0.985$  for Expt 1 and 0.978 for Expt 2) and correspondence (slope=1.02 for Expt 1 and 1.03 for Expt 2 when regressions were forced through zero).

### 4.3. Plant response

Predicted and measured predawn  $\Psi_{leaf}$  of nonirrigated millet were similar, decreasing gradually to  $-0.4$  MPa by the end of both experiments (Fig. 2). A decrease in predicted midday  $\Psi_{leaf}$  began after irrigation was terminated on the nonirrigated plots, with mid-

day  $\Psi_{leaf}$  falling to  $-1.5$  MPa in Expt 1 and  $-1.6$  MPa in Expt 2. Predicted midday  $\Psi_{soil}$  at 0.15 m declined to approximately  $-0.8$  MPa and  $-1.0$  MPa over the course of Expt 1 and 2, respectively. By contrast, there was little change in predicted midday  $\Psi_{soil}$  at 0.6 m depth until after Day 12, with  $\Psi_{soil}$  in this layer declining to  $-0.2$  MPa in Expt 1 and  $-0.4$  MPa in Expt 2.

By Day 8 to 9, measured midday stomatal conductance in the nonirrigated plots began to decrease relative to irrigated pearl millet in both experiments (Fig. 3). In the model used in this study, a decrease in simulated stomatal conductance occurs as  $\Psi_{leaf}$  approaches a critical value and declines more rapidly below this value. This decrease in stomatal conductance results in predicted transpiration decreasing relative to potential transpiration. A decline in the ratio of simulated to potential transpiration was predicted to occur by Day 9 in Expt 1 and Day 7 in Expt 2, which was similar to what was observed (Fig. 4). Thereafter, measured (with exception of Day 9 in Expt 2) and simulated transpiration rates remained below potential transpiration rates until measurements were discontinued on Day 18. By that time, there was a substantially larger difference between potential and estimated rates of transpiration in Expt 2 compared to Expt 1. After Day 9, the simulated transpiration rate was slightly greater in Expt 1 and less in Expt 2, compared to that measured.

A decrease in the ratio of estimated to potential transpiration is usually considered an indicator of stress, as is a decline in stem extension rate. In this study, measured stem extension rates in nonirrigated millet of Expt 2 decreased relative to rates in irrigated millet by Day 4, while stem extension rates in nonirrigated millet of Expt 1 never fell below irrigated millet throughout the 18-day measurement period (Fig. 5). This decline in relative rates of stem extension in Expt 2 was paralleled by a difference in surface soil temperatures between irrigated and nonirrigated plots (McIntyre et al., 1993). The temperature effect was evident on Day 4, after the irrigated plots received water on Day 3 and the nonirrigated did not (i.e., after the first differential irrigation).

### 5. Discussion

This study focused on factors limiting soil water uptake from lower depths of a drying soil. Measured

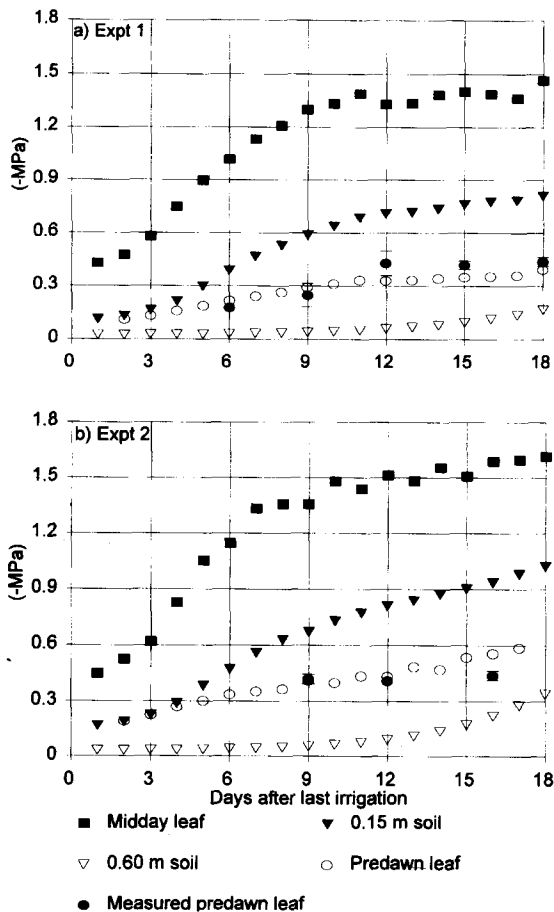


Fig. 2. Measured predawn leaf water potentials presented with simulated potentials of leaves at predawn and midday and soil water at 0.15 m and 0.60 m in Expts 1 and 2. Standard errors of measured predawn values are depicted by horizontal lines bracketing the values unless the errors are smaller than the symbols.

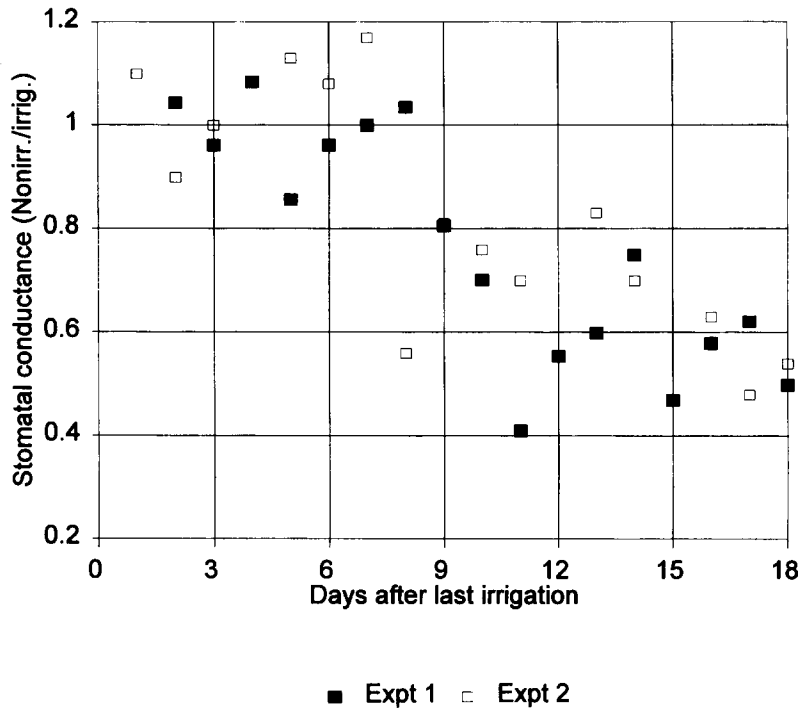


Fig. 3. Relative midday stomatal conductance (nonirrigated/irrigated) during the course of Expts 1 and 2.

and modeled results indicate that although roots were present at depths greater than 0.7 m throughout the experimental period, minimal water uptake occurred from the deeper layers. At the conclusion of both experiments, plant-available water remained at depth (approximately  $-0.03$  MPa) and yet estimated transpiration had fallen below potential by Day 9. If roots and water were present at depth, why did estimated transpiration decrease below potential transpiration?

Factors other than rooting depth capable of limiting soil water uptake include the rate of transport of water to roots (root density and/or soil hydraulic conductivity), and/or phenomena related to a decline in soil water potential. To explore the impact of these factors, simulations were repeated using data from Expt 1, but with modified values for  $L_z$ . When the  $L_z$  used in simulating Expt 1 (Simulation A) was doubled at each depth in the profile (Simulation B), similar distributions of profile water remained at the end of the simulation (Fig. 6). Total water remaining in the profile when  $L_z$  was doubled was only marginally less than that predicted in the original simulation of Expt 1 (81 mm versus 88 mm; Fig. 6). However, estimated transpiration remained within 98% of potential transpira-

tion throughout the simulated period. This indicates that merely increasing  $L$  does not necessarily result in large differences in water uptake with depth if the relative root distribution remains unchanged.

In Simulation C (Fig. 6),  $L$  was increased to  $4 \times 10^3$   $\text{m m}^{-3}$  for the layers centered at 0.9 m and 1.05 m (from  $2 \times 10^3$  and  $1 \times 10^3$   $\text{m m}^{-3}$ , respectively), whereas in shallower layers  $L$  was assigned the same value as in Simulation A. This root distribution resulted in more water uptake at depth than Simulations A or B. Total water remaining in the profile was only slightly less than Simulation A (84 mm versus 88 mm). The ratio of predicted/potential transpiration decreased below 1.0 two days later than in Simulation A and remained approximately 10% higher than Simulation A. In two additional simulations, roots were uniformly distributed throughout the profile at low ( $4 \times 10^3$   $\text{m m}^{-3}$ ; Simulation D; Fig. 6) and moderate  $L$  ( $8 \times 10^3$   $\text{m m}^{-3}$ ; Simulation E; not illustrated). In Simulations D and E,  $L$  was less than the average  $L$  ( $12 \times 10^3$   $\text{m m}^{-3}$ ) of the exponentially distributed roots in Simulation A. Both Simulations D (Fig. 6) and E resulted in more water being taken up at depth than in the previous simulations. For Simulation D, predicted tran-

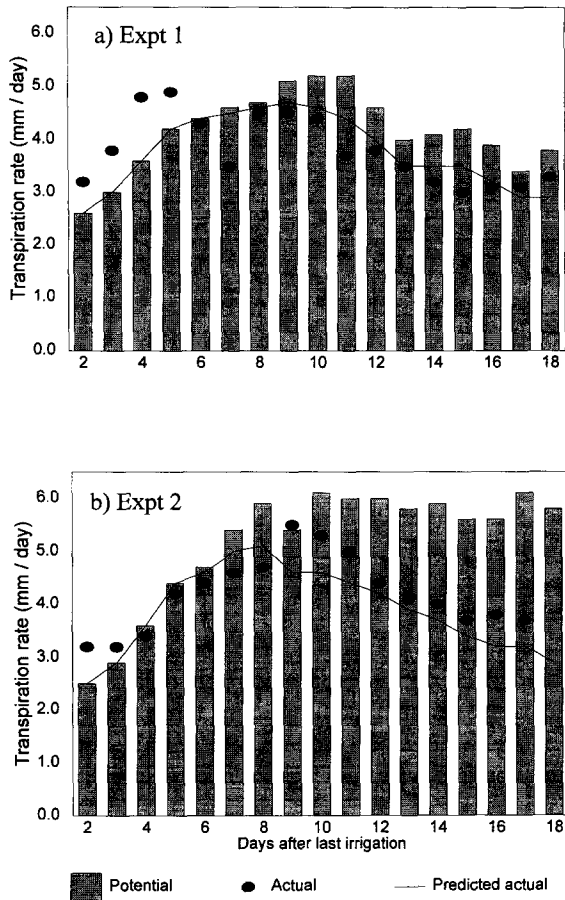


Fig. 4. Calculated potential evapotranspiration, measured transpiration, and simulated transpiration during the course of Expts 1 and 2.

spiration decreased relative to potential transpiration by the second day of the simulation and total water left in the soil profile was greater (93 mm) than in other simulations. In Simulation E, predicted transpiration did not fall below potential transpiration for the 18-d experimental period.

These analyses indicate that water uptake at depth can be enhanced by increased deep rooting or a more uniformly distributed root system. For example, root length densities below 0.6 m and plant-atmosphere conditions were the same in Simulations C and D; yet specific root water uptake was greater in Simulation C where roots were uniformly distributed throughout the profile. This implies that it is not possible to evaluate the impact of *L* on water uptake at a given soil depth without considering root distribution within the whole soil profile. In addition, model simulations indicate that

root density distribution can influence the timing and extent of a decline in transpiration relative to potential transpiration without substantial impact on total water uptake.

Monteith et al. (1989) proposed a model to examine rooting behavior and soil water uptake of crops grown on stored soil water. Their approach has been used to analyze water uptake in a range of crops (pearl millet, sorghum, chickpea and sunflower), environments (subhumid tropics to semiarid tropics), and soils (heavy clay to light sandy soils) (Robertson et al., 1993a; Meinke et al., 1993). The Monteith et al. (1989) approach assumes an apparent water extraction front characterized by a constant downward velocity closely corresponding to the rooting front. In a study of water uptake by grain sorghum, however, the water extraction front lagged behind the rooting front until a depth of approximately 1 m was reached (Robertson et al., 1993b). A similar lag phase was observed in the millet study reported here: water uptake did not immediately reflect the downward extension of roots.

In the model proposed by Monteith et al. (1989), when the extraction front arrives at a new soil layer, the water content of the layer begins to decline exponentially with time. This decline is dependent on *L* and the diffusivity of water flow to roots, and is generally held constant over the period during which water is removed from a layer. Robertson et al. (1993b) indicated that as the apparent water-extraction front descends in the soil profile, the water uptake pattern is described better by a sigmoidal function than by an exponential decay. The measured water uptake patterns reported in this study indicate a similar behavior. The Campbell potential-driven water uptake model, which assumes an exponential root distribution, well describes this pattern of a more gradual decline in water uptake with depth (Fig. 1 and Fig. 2).

Although the extraction-front model of Monteith et al. (1989) can be a useful tool for characterizing patterns of soil water uptake, the patterns observed in this study are more consistent with predictions from the potential-driven model of Campbell (1985) with a static root mass and an exponential decline in *L* with depth. In addition, the Campbell model accurately predicted the timing of stomatal closure. Such a prediction is important as a decrease in stomatal conductance can result in a reduction in water uptake.

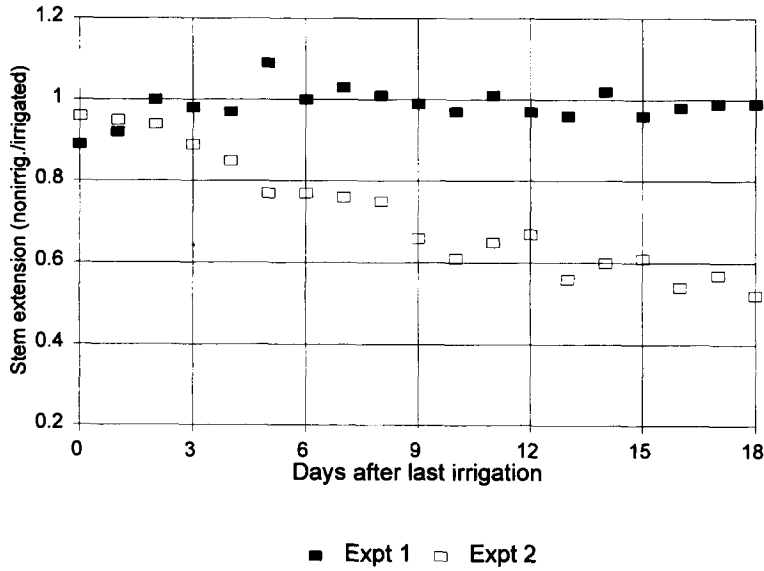


Fig. 5. The ratio of the stem + leaf extension rate of nonirrigated millet relative to irrigated millet during the course of Expts 1 and 2.

On Day 4 in Expt 2, soil water potential (as obtained from the moisture release curve) was approximately  $-0.7$  MPa in the surface  $0.15$  m, but remained less negative, (i.e.,  $> -0.1$  MPa) throughout the rest of the profile. A comparable soil water potential was

reached by Day 6 in Expt 1. Yet stomatal conductance did not decrease in either experiment until after Day 8 and stem extension did not decline throughout Expt 1. In model simulations, stomatal closure was controlled solely by leaf water potential. This indicates that sto-

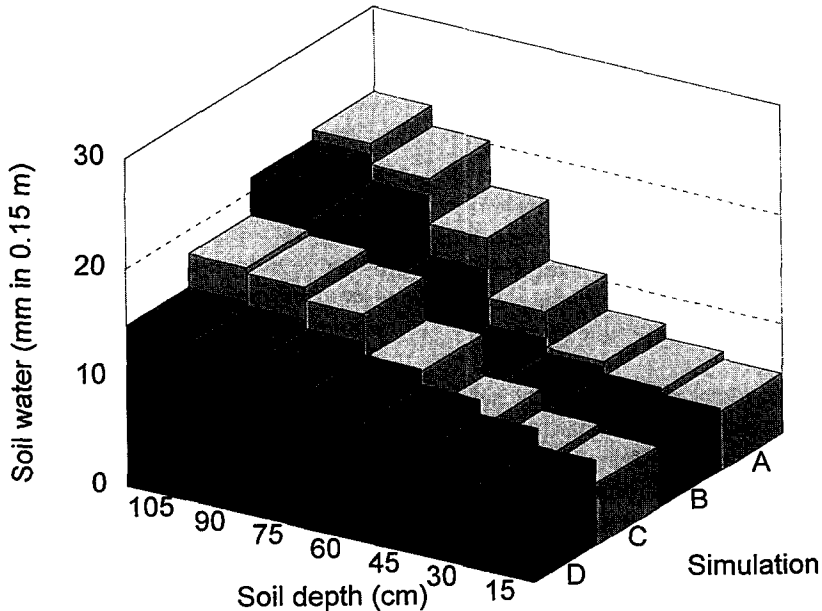


Fig. 6. Water (mm) remaining in soil profile (0.15-m increments) at end of Expt 1 under four different root density simulations: (A) exponential decline in roots with depth (B) root density used in Simulation A doubled throughout profile (C) as in Simulation A except root densities in layers centered at  $0.9$  m and  $1.05$  m increased to  $4 \times 10^3 \text{ m}^{-3}$  from  $2 \times 10^3$  and  $1 \times 10^3 \text{ m}^{-3}$ , respectively, and (D) uniform distribution of roots with depth ( $4 \times 10^3 \text{ m}^{-3}$ ).

matal closure in response to a signal generated by roots in a drying soil (Gollan et al., 1986) would be difficult to distinguish from stomatal closure stimulated by declining leaf water potential (Johnson et al., 1992).

## 6. Conclusions

A potential-driven water uptake model, which assumes a static root density exponentially decreasing with soil depth, predicted the pattern of water uptake with soil depth, the onset of a decrease in stomatal conductance, and the change in predawn  $\Psi_{\text{leaf}}$  during an 18-day drought imposed post-panicle initiation in millet growing in a semiarid climate.

The simulation model was used to analyze factors limiting water uptake at depth in the soil profile. The addition of more roots at depth increased water utilization at depth. However, the model also predicted that water uptake at depth could be enhanced by a more uniform distribution of fewer roots.

In practice, the impact of a more uniform distribution of roots would have to be considered in light of nutrient uptake and late-season use of stored soil water. In addition, the extent that improved soil management (e.g., amendments aimed at increasing soil porosity and improving soil fertility) can alter root distribution (in contrast to plant genotypic control) remains an important subject for further research.

Given the difficulties in measuring root density with depth over time and in relating root density to water uptake, simple measurements of soil water uptake patterns appear to be a more useful tool than root density measurements for evaluation of germplasm with relation to utilization of deep water.

## Acknowledgements

This research was funded in part through the Title XII Collaborative Support Program Subgrant SM-CRSP-012 from North Carolina State University. The authors would like to thank Dr. Peter Craufurd and Dr. Ken Fischer for their generous support and assistance.

## References

Barraclough, P.B. and Weir, A.H., 1988. Effects of a compacted subsoil layer on root and shoot growth, water use and nutrient

- uptake of winter wheat. *J. Agric. Sci., Camb.*, 110: 207–216.
- Buttler, I.W. and Riha, S.J., 1992. Water fluxes in Oxisols: A comparison of approaches. *Water Resour. Res.*, 28: 221–229.
- Campbell, G.S., 1985. *Soil Physics and BASIC. Transport Models for Soil-Plant Systems*. Elsevier, Amsterdam, 150 pp.
- Childs, S.W., Gilley, J.R. and Splinter, W.E., 1977. A simplified model of corn growth under moisture stress. *Trans. ASAE*, 20: 858–865.
- Cowan, I.R., 1965. Transport of water in the soil-plant-atmosphere system. *J. Appl. Ecol.*, 2: 221–239.
- Fisher, M.J., Charles-Edwards, D.A. and Ludlow, M.M., 1981. An analysis of the effects of repeated short-term soil water deficits on stomatal conductance to carbon dioxide and leaf photosynthesis by the legume *Macropitium atropupureum* cv. Siratro. *Aust. J. Plant Physiol.*, 8: 347–357.
- Gardner, W.R., 1965. Dynamic aspects of soil-water availability to plants. *Ann. Rev. Plant Physiol.*, 16: 323–342.
- Gerwitz, A. and Page, E.R., 1974. An empirical mathematical model to describe plant root systems. *J. Appl. Ecol.*, 11: 773–464.
- Gollan, T., Passioura, J.B. and Munns, R., 1986. Soil water status affects the stomatal conductance of fully turgid wheat and sunflower leaves. *Aust. J. Plant Physiol.*, 13: 459–464.
- Hamblin, A. and Tennant, D., 1987. Root length density and water uptake in cereals and legumes: How well are they correlated? *Aust. J. Agric. Res.*, 38: 513–527.
- Johnson, I.R., Melkonian, J.J., Thornley, J.H.M. and Riha, S.J., 1992. A model of water flow through plants incorporating shoot/root 'message' control of stomatal conductance. *Plant Cell Environ.*, 14: 531–544.
- Jordan, W.R. and Miller, F.R., 1980. Genetic variability in sorghum root systems: Implications for drought tolerance. In: N.C. Turner and P.J. Kramer (Editors), *Adaptation of Plants to Water and High Temperature Stress*. John Wiley, New York, pp. 383–399.
- Kowal, J.M. and Knabe, D.T., 1972. *An Agroclimatological Atlas of the Northern States of Nigeria*. Ahmadu Bello Press, Samaru-Zaria, Nigeria, 111 pp.
- McIntyre, B.D., 1992. *Water use in cereal crops in the semiarid tropics*. PhD Dissertation, Cornell University, Ithaca, NY.
- McIntyre, B.D., Flower, D.J. and Riha, S.J., 1993. Temperature and soil water status effects on radiation use and growth of pearl millet in a semiarid environment. *Agric. For. Meteorol.*, 66: 211–227.
- Meinke, H., Hammer, G.L. and Want, P.J., 1993. Potential soil water extraction by sunflower on a range of soils. *Field Crops Res.*, 32: 59–81.
- Monteith, J.L., Huda, A.K.S. and Midya, D., 1989. RESCAP: A resource capture model for sorghum and pearl millet. In: S.M. Virmani, H.L.S. Tandon and G. Alagarswamy (Editors), *Modeling the Growth and Development of Sorghum and Pearl Millet*. Research Bull. No. 12, ICRISAT, Patancheru, India, pp. 30–38.
- Passioura, J.B., 1983. Roots and drought resistance. *Agric. Water Manage.*, 7: 265–280.
- Robertson, M.J., Fukai, S., Ludlow, M.M. and Hammer, G.L., 1993a. Water extraction by grain sorghum in a sub-humid environment. I. Analysis of the water extraction pattern. *Field Crops Res.*, 33: 81–97.

Robertson, M.J., Fukai, S., Ludlow, M.M. and Hammer, G.L., 1993b. Water extraction by grain sorghum in a sub-humid environment. II. Extraction in relation to root growth. *Field Crops Res.*, 33: 99–112.

Stockle, C. and Campbell, G.S., 1985. A simulation model for predicting the effect of water stress on yield: An example using corn. *Adv. Irrigation*, 3: 283–323.